Determination of a critical separation concentration for associative polymers in porous media based on quantification of dilute and semi-dilute concentration regimes.

AFOLABI, R.O., OLUYEMI, G.F., OFFICER, S. and UGWU, J.O.

2020

Research Article

Title: Determination of a Critical Separation Concentration for Associative Polymers in Porous Media Based on Quantification of Dilute and Semi-Dilute Concentration Regimes.

Authors: Richard O. Afolabi[1,] *, Gbenga F. Oluyemi[1], Simon Officer[2], Johnson O. Ugwu[3].

Affiliations: [1] Petroleum Engineering Research Group (PERG), School of Engineering, Robert Gordon University, Aberdeen, AB10 7GJ, United Kingdom.

[2] School of Pharmacy and Life Sciences, Robert Gordon University, Aberdeen, AB10 7GJ, United Kingdom.

[3] School of Science, Engineering and Design, Teesside University, Middlesbrough, Tees Valley, TS1 3BX, United Kingdom.

***Contact email**: r.afolabi@rgu.ac.uk

Abstract

Hydrophobic interactions are an inherent property of associative polymers which results in the formation of molecular aggregates. The loss of hydrophobic interactions under reservoir conditions have been reported, and this results in increased fluid – rock interaction effect such as adsorption. However, existing adsorption studies only reports the interaction of individual molecules with rock surface without taking into account mechanically retained molecular aggregates in narrow pores. The implication of this is a reduction in associative effect between polymer molecules during transport in a porous media. In this work, the minimization of this phenomenon and sustenance of the interaction network was studied through a theoretically defined dimensionless parameter for the quantification of molecular interactions in the various polymer concentration regimes. It was established in this work that

associative polymers exhibit a critical separation concentration during propagation in a porous media under given reservoir conditions. This critical separation concentration marks the concentration beyond which large molecular aggregates constituting the hydrophobic network is sterically excluded and retained in narrow pore spaces. This separation phenomenon was predicted to occur when the proportion of molecular interactions arising from hydrophobic and intramolecular interactions are equal. Thus, the balance in the molecular interactions in the semi – dilute concentration regime was identified as key in minimizing the loss of hydrophobic interactions to aggregate retention and optimizing its sustainability in a porous media. Consequently, a novel approach was developed based on this knowledge for the transport of associative polymers at which these hydrophobic interactions are sustained. It was demonstrated that propagating associative polymers using this approach ensured the sustainability at concentrations below the critical separation concentration tend to maximize the hydrophobic interaction network with minimal loss of polymer chains retention mechanisms.

Keywords: Polymers; Hydrophobic Interactions; Chemical Flooding; Optimization

1. Introduction and Theoretical Assumptions

The viscosity of associative polymers is predominantly a function of the hydrophobic interaction network that exists between polymer chains (Yang et al., 2016). The identification of a parameter that uniquely describes these hydrophobic interactions between associative polymers is crucial in the understanding of its sustainability, optimization and control when transported in a reservoir. This parameter is particularly significant, as associative polymers prepared at surface conditions would behave differently when injected into subsurface formation with high salinity and temperature (Ye et al., 2013; Chen et al., 2016; Zhang et al., 2019). In other words, the hydrophobic interaction network is subject to *in-situ* variation depending on the extent to which the subsurface conditions differ from the surface conditions of preparation (Sun et al., 2015; Gou et al., 2015; Zhong et al., 2018; Li et al., 2018; Afolabi & Yusuf, 2019). Furthermore, the variation of hydrophobic interaction is also affected by the phenomenon of rock adsorption and retention. The adsorption of polymer chains on rock surfaces has been shown to increase with polymer concentration. The critical aggregation concentration (CAC) remains the only intrinsic property by which hydrophobic interactions (intermolecular association) can be distinguished from intramolecular interactions (Liu et al., 2014; Quan et al., 2016; Khan and Brettmann, 2019). The critical aggregation concentration is the critical concentration beyond which individual polymer molecules in solution begin to form molecular aggregates due to hydrophobic interactions. Consequently, the CAC distinguishes the dilute concentration regime from the semi-dilute/concentrated regime. In the dilute regime, individual polymer molecules are isolated from each other in solution and as such, the hydrophobic blocks on the molecules interact with each other within the molecules hence the concept of intramolecular interaction. At polymer concentration above the CAC (semi – dilute regime), the associative (hydrophobic) characteristics of the polymer come into

effect. At this point, the network of hydrophobic interactions within the polymer solution is initiated with the associative effect starting from the polymer chain with a large hydrophobic block down to the chains with small hydrophobic blocks. Likewise, at polymer concentration below the CAC (dilute regime), intramolecular association within polymer chains become dominant. Here, associative polymer chains are distinctively independent of each other with interaction within the polymer chains. Apparently, it has also been established from previous studies that the CAC of associative polymers responds to changes in temperature and brine salinity (Afolabi, 2015; Sun et al., 2015; Afolabi et al., 2019a; Afolabi et al., 2019b). Accordingly, the change in the CAC of associative polymers was employed in the estimation and quantification of changing hydrophobic interactions between polymer chains. However, the CAC of associative polymers does not indicate the separation and hydrodynamic retention of polymeric hydrophobic aggregates which is a common observation during flow in a porous media. This segregation result in the injected concentration being split into three phases: a polymer – rich phase, a polymer – depleted phase and a solvent (water) phase. The solvent phase, being propagated at a low flowrate, will occupy the micropores of the porous media that are inaccessible to the polymer molecules. In the case of the polymer – depleted phase, this fills the pore surface and represents practically the immobile phase of the polymer solution. Individual polymer molecules in this phase practically interact with the rock surface resulting in polymer adsorption. Finally, the polymer – rich layer is sterically excluded from the remaining two layers to flow at the centre of the pores. This rich layer remain the exclusive preserve of polymeric hydrophobic interactions. This observed phenomenon arises due to the size distribution of the polymer molecules in solution. The sterically excluded polymer – rich phase occurs due to hydrophobic interactions that exist between polymer chains with larger hydrophobic blocks on their backbone. As such, the network of polymer molecular aggregates that constitute this phase flow as a single entities in the porous media.

Furthermore, the segregation and retention of some polymer aggregates during flow in porous media explains why the effective viscosities measured during core floods may be lower than the pre – injection viscosity value. More so, the segregation of polymer molecules means that the injected associative polymer solutions exhibit an *in-situ* concentration (or effective polymer concentration). Therefore, an innovative approach was developed towards the determination of a critical separation concentration towards distinguishing polymer aggregates available for flow in near the centre of the pores and those available for retention in the narrow pore spaces. The knowledge of the dynamics of this critical separation concentration in conjunction with the CAC of associative polymers would further assist in the design and optimizing of polymer flooding operations towards the sustainability of these hydrophobic interactions under reservoir conditions.

1.1. The Proportion of Hydrophobic Interactions in Semi-Dilute Regime

In defining a parameter that quantifies the proportion of hydrophobic interactions between associative polymer chains at a given condition of temperature and salinity, the following assumptions were made:

a) The summation of the proportion of molecular interactions (hydrophobic and intramolecular) arising from polymer chain interaction that constitutes the semi – dilute concentration regime is assumed to be unity.
b) Intramolecular interaction takes place both in the dilute regime (C_p less than the critical aggregation concentration, C_C) and the semi – dilute regime (C_p greater than the critical aggregation concentration, C_C).
c) The hydrophobic interaction network between polymer chains only takes place in the semi – dilute concentration regime, i.e. polymer concentration,C_p must be greater than the critical aggregation concentration, C_C.

d) The increase in polymer concentration, C_p (beyond C_c) would lead to a rise in the proportion of hydrophobic interactions and a reduction in the proportion of intramolecular interactions.

e) The separation of polymer molecular aggregates would only take place in the semi – dilute regime when hydrophobic interactions dominates over intramolecular interactions.

Based on the assumptions highlighted above, the following dimensionless parameter, I_{sd} was used to quantify the hydrophobic interactions between associative polymer chains at a given condition of temperature, T and salinity, B_s in (1):

$$(I_{sd})_{T,B_s} = \frac{C_p - (C_c)_{T,B_s}}{C_p} \begin{cases} C_p > C_c \\ C_c \neq 0 \end{cases} \quad (1)$$

The proportion of intramolecular interactions, I_d in the semi – dilute reime at given reservoir conditions of temperature, T and brine salinity B_s can be estimated based on assumption (b) as shown in equation (2):

$$(I_d)_{T,B_s} + (I_{sd})_{T,B_s} = 1 \quad (2)$$

Simplifying equation (2) gives (3)

$$(I_d)_{T,B_s} = \left[\frac{(C_c)_{T,B_s}}{C_p}\right] \begin{cases} C_p > C_c \\ C_c \neq 0 \end{cases} \quad (3)$$

1.2. The Proportion of Intramolecular Interactions in the Dilute Regime

The proportion of intramolecular interactions, I_d in the dilute regime at given reservoir conditions of temperature, T and brine salinity B_s can be estimated from equation (4):

$$(I_d)_{T,B_s} = \left[\frac{C_p}{(C_c)_{T,B_s}}\right] \begin{cases} C_p < C_c \\ C_c \neq 0 \end{cases} \quad (4)$$

Since intramolecular interactions dominates in this regime, the assumption of summative effect of molecular interactions considered in the semi – dilute regime does not apply here.

1.3. Critical Separation Concentration, $C_{p,opt}$

Based on the assumption made in (e) above, the balance in the proportion of molecular interactions in the semi – dilute regime is considered as the point where $(I_{sd})_{T,B_s}$ is equal to $(I_d)_{T,B_s}$ as shown in (5)

$$(I_{sd})_{T,B_s} = (I_d)_{T,B_s} \quad (5)$$

This point of equilibrium was employed in the determination of the critical separation concentration. The validation of this prediction was carried out using static and dynamic adsorption experiment in a porous media. The adsorption isotherms were studied and the point where there is a deviation from the known polymer isotherm patterns was identified as the point where retention is a combination of adsorbed polymer molecules and hydrodynamically trapped molecular aggregates.

2. Methodology

2.1. Materials: Associative Polymer and Salts

The hydrophobically associating polymer (Superpusher D118; Degree of hydrolysis = 25 – 30 mol % at 25 ^{0}C; $\bar{M}_w$ = 16 – 20 x 10^6 g/mol; Appearance = white granular solid; Hydrophobe content = medium; Total anionic content = 15 – 25 mol.%) employed in this study was manufactured and supplied by SNF Floerger, ZAC milieux, 42163 Andrezieux (France). The salts employed in the preparation of synthetic formation brine (SFB) include analytical grade Sodium Chloride (NaCl), Magnesium Chloride ($MgCl_2$), Calcium Chloride ($CaCl_2$), Potassium Chloride (KCl), Sodium Sulphate (Na_2SO_4), Sodium Hydrogen Carbonate ($NaHCO_3$) and Strontium Chloride ($SrCl_2$). These salts were purchased from Sigma Aldrich (UK) with the properties as provided by the supplier.

2.2. Preparation of Synthetic Brine, Stock and Dilute Polymer Solutions

Synthetic brine was formulated by dissolving varying amounts of salts in deionized water. The water was deionized to a resistivity value of 18 MΩ-cm (a threshold for removal of ions) using a Millipore™ pumping unit. The brine solutions were prepared to contain both NaCl and $CaCl_2$ in the ratios 10 to 1, respectively. Table 1 presents the number of salts used the preparation of the synthetic brine used for rheological analysis. Before use, the synthetic brine solution was filtered through a 0.22 μm filter paper to ensure the removal of any particles present. Stock polymer solution (Concentration: 5000 ppm) was prepared by dissolving polymer granules in the synthetic brine. To ensure complete dissolution, the polymer-brine mixture was stirred for 2 days using a Fischer Scientific magnetic stirrer (Model: 11-102-50SH) and allowed to hydrate for a further 24 hours. The diluted polymer solutions were prepared freshly according to the API specification RP – 63 (Recommended Practices for Evaluation of Polymers for Enhanced Oil Recovery). The concentrations of the dilute polymer solutions used for this study include the following: 10, 50, 100, 300, 500, 750, 1000 ppm. Table 2 shows the calculation procedures in the preparation of the stock and diluted polymer solutions according to API specification RP – 63.

2.3. Rheological Measurement of Polymer Systems

Measurement of the polymer viscosity was carried out using a Brookfield Digital Rheometer (Model DV-III) for low shear rates (Speed Range: 0 – 200 RPM with 0.1 RPM increments; Temperature sensing range: - 100 °C to 300 °C). The Fann Viscometer (Model 35A/SR-12) was used for high shear rates (pre – set rates: 600, 300, 200, 180, 100, 90, 60, 30, 6, 3, 1.8, 0.9 RPM; Temperature range: 5 °C to 40 ^{0}C). The temperature of the polymer solutions (Temperatures: 25, 50, 75, and 85 ^{o}C) was adjusted by circulating water on the outer jacket of the viscometer cup containing the solution using the Medline Refrigerating & Heating Bath Circulator (Model: RW – 0525G) was used for the temperature control.

2.4. Adsorption Study in Porous Media

2.4.1. Static Adsorption Test

100 g of the commercial silica sand was weighed into a 500 ml sample bottles. 400 g of polymer solutions (10, 50, 100, 300, 500, 750, 1000 ppm) was added to each of the sample bottles containing the silica sands. The containers were caped and stored at representative temperatures for two days. The vessels were agitated periodically to maintain good contact between the polymer solutions and the silica sands. The polymer solutions were separated from the silica sands by filtering through a 10-micron filter. The final concentrations of the polymer solutions were estimated from viscometry using an Ubbelohde viscometer. The adsorbed polymer was calculated using equation (6) below:

$$C_{ad} = \frac{W_p(C_i - C_f)}{W_s} \quad (6)$$

Where C_{ad} is the amount of polymer adsorbed, W_p is the weight of polymer solution, W_s is the weight of the silica sand, C_i and C_f is the initial and final polymer concentration respectively. Two commercial silica sands codenamed 40/60 and P230 were applied in the adsorption study. The properties of these sands and concentration of salts used are summarized in Table 3.

2.4.2. Dyanamic Adsorption Test

Figure 1 show a simplified diagram of the flow system used for conducting dynamic adsorption studies under different flow conditions. The flow system consist of a snd – pack holder or stainless steel core holder with length of 25 cm, internal diameter of 5.067 cm and cross sectional area of 20.16 cm^2. A high performance syringe pump (HPLC 1500; Max Pressure: 6000 psi) was used to deliver varying fluid volume af different rates (Max. rate: 12 ml/min). Data aqisition was provided using a high speed National Instruments Data Acquisition System (NIDAQ) through pressure transducer (0 – 30 psi) mounted across the

core. This ensures that pressure monitoring and measurements from connected transducers were digitised and logged to a personal computer. A transducer demodulator used to provide the correct sensor excitation and demodulate the returned alternating current signal from the sensor into a $+/-10V$ direct current signal appropriate for the data acquisition system. The procedure for the dynamic adsorption test is as follows:

a) The pump in the flow system was set to the required injection rate (0.5 ml/min) and synthetic brine (4.2 %TDS) was injected until the pressure stabilized;

b) Polymer injection of the desired concentration (100 ppm) (**first polymer bank**) was started at the same flow rate (0.5 ml/min) until the pressure stabilized after injection of about 3 PVs;

c) 10 PVs of brine (4.2 %TDS) was injected to flush out all non – adsorbed polymer molecules present in the sand – packed core.

d) The pump rate was adjusted (1.5 and 3 ml/min) and the process of polymer injection into the sand – packed media was repeated until pressure stabilization was achieved after which step (c) was repeated to flush out non – adsorbed polymer molecules.

e) Effluent polymer cuts from the dynamic flow system were collected at regular time intervals in test tubes and marked to record events of the fluid and rate changes where necessary;

f) Polymer retention was estimated by comparing the plot of effluent concentration curves against pore volume for 0.5 and 1.5 ml/min; 0.5 and 3 ml/min respectively.

g) To obtain polymer retention isotherms, Steps (a) – (f) were repeated for any increasing polymer concentrations (**subsequent polymer banks**) and the concentration point beyond

which there is a rapid increase in the polymer adsorption was determined and this corresponds to $C_{p,opt}$.

3. Results and Discussion

3.1. Determination of the Critical Aggregation Concentration

Polymer rheology which involved the determination of viscosity for different polymer concentrations at a given was determined as described in the methodology above. The plot of polymer viscosity against concentration under different temperatures are contained in Figure 2. From Figure 2, it can be observed that in both low and high concentration regions, a linear relationship exists between the polymer viscosity and concentration. For the low concentration region, a closer observation as concentration increases from zero upwards indicates that at a particular concentration, there is a deviation from linearity. Similarly, observing the high concentratin region as the polymer concentration decreases from a value of 5 g/L, a point is also reached where there is a deviation from linearity. The deviation in linearity is an indication of a change in the nature of molecular interactions which exists between polymer molecules. The point where there is a deviation from linearity in both regions is considered as the critical aggregation concentration. This point is considered the critical aggregation concentration because it essentially describes the point where there is a deviation from an initial polymer character in solution described by the linear trend previously observed to a new behaviourial trend which is evident from the new linear trend in the high concentration region. In other words, beyond this point there is a rapid change in rheological behaviour marked with a rapid rise in polymer viscosity. This point was determined by fitting two linear models of the form shown below in equation (7) to the low and high concentration regions

$$\mu_p = aC_p + b \qquad (7)$$

Where μ_p is the polymer viscosity, C_p is the polymer concentration and a, b are model constants respectively. Two linear models of the form in (7) were fitted via regression analysis to the regions (dilute and semi-dilute region) which approximates a straight line in the plot of viscosity against polymer concentration. The critical concentration was approximated as the point of intersection of the fitted linear models. Figure 2 shows the approach taken for the determination of the critical concentration of the associative polymer under different temperatures (25, 50, 75 and 85 ^{0}C). It can be observed that the critical concentration increased with temperature from 25 to 85 ^{0}C as shown in Figure 3. This increment signifies a change in the associative characteristics of the polymer through the transition of polymer chains from the hydrophobic network to the dilute concentration regime. Previous studies on associative polymers have also reported a similar result of critical concentration and temperature (Sun et al., 2015). Consequently, the region for dilute behaviour increase due to the loss of hydrophobic interactions starting with the shorter polymer chains containing small hydrophobic areas. Similarly, the critical concentration was also determined for the associative polymer under different percent dissolved solids (3.6, 3.8,
4.0 and 4.2 % TDS) as shown in Figure 4. The approach also involved the use of two linear models fitted via regression analysis to the regions (dilute and semi-dilute region) which approximates a straight line in the plot of viscosity against polymer concentration. It can be observed that the critical concentration increased minimally with the percent dissolved solids (Figure 5). It could be said that the loss of polymer chains from the semi-dilute regime to dilute regime takes place gradually under the effect of dissolved solids than temperature.

3.2. Polymer Viscosity

3.2.1. Effect of Temperature

Figures 6a – d show the variation of the polymer viscosity with shear rate at different tempratures under given conditions of total dissolved solids. In order to study the effect of

temperature on the polymer viscosity, lowest shear rate approximating zero-shear rate was considered. The lowest shear rate obtainable from the Rheometer was considered to approximate zero-shear condition and the viscosity vale taken at this rate (zero-shear viscosity). The changes in the approximate zero-shear viscosity with temperature was observed at each given condition of total dissolved solids. At 3.6 and 3.8 % TDS, the decrease in the values of the zero-shear viscosity of the polymer solution with temperature follows an approximately linear trend up to 75 ^{0}C (Figure 6a and 6b). A similar linear pattern with the zero-shear viscosity was obtained at 3.8 % TDS, but it was observed that there was a dip at 50 ^{0}C (Figure 6b). However, this trend was not the case at 4.0 and 4.2 % TDS, respectively. Here, the zero-shear viscosity decrease was gradual with an increase in temperature up to 75 ^{0}C. Between temperatures 50 and 75 ^{0}C, there is a stable trend in the zero-shear viscosity with temperature (Figures 6c and 6d). However, beyond this temperature in all instances, there was a further decline in the zero-shear viscosity of the associative polymer. The various trend explained is summarized in Figure 6e. When the thermal energy acquired by a given polymer chain exceeds its bond energy in the hydrophobic interaction network, the chain breaks off from the network and polymer viscosity is reduced. The gradual increase in the thermal energy of the polymer chains starts with the ones with shorter hydrophobic blocks up to the longer chains.

3.2.2. Effect of Total Dissolved Solids (TDS) and Polymer Concentration

Figures 7a – d show the variation of the polymer viscosity with shear rate at different total dissolved solids under given conditions of temperatures. Similar to the effect of temperature, the changes in the approximate zero-shear viscosity with the total dissolved solids was observed at each given condition of temperature. The obtained trend from the effect of total dissolved solids on the polymer viscosity at shear rate approximating zero-shear rate is summarized in Figure 7e. At 25 and 50 ^{0}C, the effect of metal ions present in solutions is very

evident on the zero-shear viscosity, which shows a rapidly decreasing trend. Increase in the presence of salt ions has a profound effect on the zero-shear viscosity of the associative polymers at a given temperature condition. However, at temperatures of 75 and 85 ^{0}C, the rate of zero-shear viscosity decline with the concentration of dissolved solids is reduced compared to the previous two temperature values earlier discussed. Also, the zero-shear viscosity of the polymer seems to be higher at 4.2 % TDS for the trend at 75 ^{0}C compared to 50 ^{0}C. This trend further indicates the salt tolerance of associative polymers; however; the response of this associative polymer is a function of the combination of the studied factors. The effect of polymer concentration on the viscosity of associative polymers stems from the interpenetration of polymer chains which allows for the interaction of hydrophobic blocks on the polymer chains. Figures 2 and 4 show the response of polymer viscosity to concentration at varied temperature and salinity conditions.

3.3. Determination of Critical Separation Concentration

The intramolecular interactions, I_d increase with polymer concentration up to the critical aggregation concentration as shown in Figure 8 for conditions of 25 ^{0}C (3.6 % TDS), 50 ^{0}C (3.8 % TDS) and 75 ^{0}C (4.0 % TDS) respectively. This increment indicates the increment in the number of polymer chains with concentration. However, this parameter decreased with polymer concentration beyond the critical aggregation concentration, indicating the onset of the propagation of hydrophobic interaction between polymer chains. For the studied conditions of 25 ^{0}C (3.6 % TDS), 50 ^{0}C (3.8 % TDS) and 75 ^{0}C (4.0 % TDS), it was observed that the broadness of these plots of I_d increased with these conditions. This broadness indicates the variation (increment) in the intramolecular behaviour with temperature. It would be observed that the peak of the I_d curve shifted to the right with temperature indicating an increase in the intramolecular behaviour in the dilute and semi – dilute concentration regimes. However, the I_{sd} plot show a downward decrease with temperature indicating a decrease in

hydrophobic interactions in the semi – dilute regime. In other words, the plot of I_d effectively describe polymer intramolecular behaviour in the dilute and semi – dilute concentration regimes. Furthermore, Figure 8 shows the plots of the hydrophobic interactions, I_{sd} against polymer concentration up to 5 g/L at conditions of 25 ^{0}C (3.6 % TDS), 50 ^{0}C (3.8 % TDS) and 75 ^{0}C (4.0 % TDS) respectively. For an associative polymer prepared at a condition of 25 ^{0}C (3.6 % TDS), the proportion of hydrophobic interaction present amount to 0.90 (or 90 % of all molecular interactions) at a concentration of 5 g/L. However, when exposed to a different temperature and salinity condition of 50 ^{0}C and 3.8 % TDS, the proportion of hydrophobic interactions decreased from 0.90 to 0.85. This decrease suggests that 0.05 or 5 % of hydrophobic interactions were lost under these conditions. Similarly, at a different temperature and salinity condition of 75 ^{0}C and 4.0 % TDS, the proportion of hydrophobic interactions decreased from 0.90 to 0.66 indicating 0.24 (or 24 %) of hydrophobic interactions were lost as also shown in Figure 8. Equally, the decreasing values for hydrophobic interactions can also be observed at other given polymer concentration values at 50 ^{0}C (3.8 % TDS) and 75 ^{0}C (4.0 % TDS) respectively. In addition, the onset of hydrophobic interactions was observed to increase from 0.49 (25 ^{0}C and 3.6 % TDS) to 0.75 g/L and 1.7 g/L for the conditions at 50 ^{0}C (3.8 % TDS) and 75 ^{0}C (4.0 % TDS) respectively. It would be observed that the plots for I_{sd} and I_d intersect at approximately 0.5 respectively and the estimated polymer concentration, $C_{p,opt}$ at this point of intersection was 1 g/L (or 1,000 ppm), 1.7 g/L (1700 ppm) and 3.3 g/L (3300 ppm) at 25 ^{0}C (3.6 % TDS), 50

^{0}C (3.8 % TDS) and 75 ^{0}C (4.0 % TDS) respectively. This estimated polymer concentration is the critical separation concentration at which there is a balance in molecular interactions (hydrophobic and intramolecular interactions) under the given conditions. The increase in this critical separation concentration of the associative polymer is evident of the changing conditions of temperature and salinity. The significance of this novel approach is the control

and monitoring of hydrophobic interactions under different reservoir conditions, and this is adjusted for in the required polymer concentration. This significance is summarized by considering three case scenarios. Firstly, polymer concentration less than the critical aggregation concentration and the critical separation concentration ($C_p < C_{p,opt} < CAC$). This scenario marks the absence of hydrophobic interactions among polymer chains in solution. The propagation of polymer solutions under these conditions would see polymer molecules interacting with the rock surface without sufficient viscosity for mobility control. Secondly, the scenario where polymer concentration is greater than the critical aggregation concentration but less than the critical separation concentration ($C_{p,opt} > C_p > CAC$). In this scenario, hydrophobic interactions exist between polymer molecules and the propagation of these molecules would result in hydrophobic interactions not lost to any retention mechanism asides adsorption. Here, hydrophobic interactions would be sufficient to provide the needed mobility control during EOR. Thirdly, polymer concentration is higher than the critical aggregation concentration and the critical separation concentration ($C_p > C_{p,opt} > CAC$). Operating at these conditions would mean that there would be insufficient hydrophobic interactions propagated through the porous media. In addition to polymer molecules lost to fluid – rock interactions phenomenon such as adsorption, molecular aggregates arising from hydrophobic interactions are also lost to different entrapment mechanism. Therefore, the second scenario depicts that the application of associative polymers goes beyond operating above the critical aggregation concentration but also ensuring that the injection concentration is below the critical separation concentration. This ensures that there are sufficient hydrophobic interactions for mobility control while minimizing the effect of polymer loss arising from hydrodynamically induced retention.

3.4. Polymer Adsorption Study

In validating the outcome for the critical separation concentration, a static adsorption study of the associative polymer using commercial silica sands described in Table 3.

3.4.1. Static Adsorption Isotherms and Model Prediction

Figure 9 shows the adsorption isotherms after contacting the associative polymer with different silica sands. In Figure 9a, it was observed that the adsorption isotherm show a rapidly increasing value beyond a particular concentration which corresponds approximately to 300 ppm (0.3 g/L). This trend deviates from known adsorption isotherms where adsorption reaches a maximum value as concentration increases. Adsorption isotherms are known to explain how individual polymer molecules interact with the solid surface. However, the formation of molecular aggregates have been reported with hydrophobically associating polymers which gives rise to molecular sizes which may be greater than that reported for individual polymer molecules. In other words, known adsorption isotherm models do not capture the effects of molecular aggregates arising from hydrophobic interactions. The rapid increase reported from Figure 9 would only indicate the effect of other retention mechanism arising from molecular aggregates asides adsorption. This isotherm in Figure 9 was compared with the prediction using the graphical illustration obtained using the equations (1) to (4). Figure 10a shows the graphical trend for the prediction using equations (1) to (4) for the 40/60 silica sand. It was observed that the point of intersection was approximately 300 ppm (0.3 g/L), which corresponds to the value obtained from the adsorptions isotherm. This further indicates that other retention mechanism asides adsorption would take place when hydrophobic interactions are dominant over intramolecular interactions. This explains why the critical separation concentration would always be higher than the critical aggregation concentration. Furthermore, the critical separation concentration would only be possible when the critical aggregation concentration is exceeded. Mathematically, equation (8) shows

the relationship between the critical separation concentration concentration, $C_{p.opt}$ and the critical aggregation concentration, C_c

$$C_{p.opt} = 1.99272C_c \quad (8)$$

The equation in (8) applies the 40/60 silica sand within the temperature constraints of 25 – 75 ℃ and salinity condition of 4.2 %TDS (Na^+: $Ca^{2+} - 10$: 1). From the expression in (8), the absence of hydrophobic interactions ($C_c = 0$) would imply that the formation of molecular aggregates would not take place. Similarly, the adsorption trend was the same using a different silica sand (P230) however, the point of critical separation concentration was obtained at a higher concentration value of 500 ppm (0.5 g/L) (Figures 9b and 10b). These observed trends with different silica sands show the effect of formation properties such as porosity. For low porosity values, there is more polymer molecules associated with the rock surface, as flow near the centre of the pores is limited. However, for high porosity values, there are fewer polymer molecules related to the rock surface and more polymers flowing at the centre of the pores. This observation explains why the critical separation concentration is at a higher value for P230 than the 40/60 silica sand. The reported results in this section were

based on static conditions in which the effects of flow conditions are absent. Therefore, the critical separation concentration value may be subject to change under hydrodynamic conditions as reported under dynamic adsorption study.

3.4.2. Polymer Re-Adsorption and Model Prediction

Figure 11 shows the polymer re – adsorption process carried out by contacting 1000 ppm of polymer solution with already contacted sand. Contacting the previously adsorbed sand with a polymer solution with a concentration above the critical separation concentration show that the amount of polymer adsorbed was approximately constant up to the critical concentration. This observation was the case for both silica sands considered in the adsorption study. This

show that there is a given amount of polymer molecules which constitute what would interact with polymer rock surface and molecular aggregates whose size is too large to be propagated through narrow pores and therefore would be hydrodynamically retained. It further indicates that beyond the critical aggregation concentration, associative polymers exhibit a critical separation concentration, which gives an idea of the proportion of molecular aggregates that would be sterically excluded from the hydrophobic interaction network in solution flowing at the centre of the pores.

3.4.3. Dynamic Adsorption Study

Figure 12 show the effect of flow conditions on the adsorption of associative polymers in the porous media. Operating at a low flow rate, polymer adsorption is higher and at high flow rate, polymer adsorption was lower. However, comparison with the static adsorption isotherm indicates that the dynamic conditions effected low adsorption isotherm. The low adsorption isotherms under dynamic conditions arise due to the reduced contact time available for polymer molecules to interact with the solid surface. The available contact time for polymer molecules increase with reduced flow rate. However, dynamic adsorption in a porous media is a complex phenomenon to understand compared with static adsorption process. In addition, the disaggregated nature of the sand grains under static adsorption test ensure that the exposed surface area per volume is higher compared to the compacted sand grains under dynamic conditions which ensures that exposed surface area per volume is minimal. Furthermore, the effect of inaccessible pore volume ensure that accelerates the flow of polymer solution in the porous media ensuring that the polymer molecules have less contact time with the rock surface. The critical separation concentration of the associative polymer under dynamic conditions was observed to occur at higher polymer concentrations compared to the static adsorption isotherm. The effect of shear rate on the critical separation concentration is explained by visualizing these polymer chains as both entangled and single-

independent coils, and when subjected to flow, two competing forces arise. Firstly, the entropic force maintains the existing polymer configuration. For the single-independent coils, this entropic force keep the polymer chains independent from each other. On the other hand, the magnitude of the entropic force on the molecular aggregates is a function of hydrophobic interaction between polymer molecules. The existing polymer configuration eventually give rise to the critical separation concentration under these conditions. Secondly, a drag force comes into play when subjected to flow conditions. This drag force arise from the interaction between polymer molecules and the solvent in which it is dissolved. The drag force ensure that the independent polymer chains are aligned in the flow direction thereby minimizing contact time with the solid surface. However, in the case of the molecular aggregates, the drag force tries to disentangle the associated polymer molecules in addition to aligning them in the flow direction. For molecular aggregates disentangled and aligned in the flow direction, they become independent chains. As a result, the critical separation concentration of the associative polymer increases with flow rate indicating a reduction in the size of molecular aggregates in the polymer solution.

Conclusion and Future Perspectives

The sustainability of hydrophobic interactions between associative polymer chains is primarily a function of the balance between the molecular interactions arising from the hydrophobic effect in the semi-dilute regime and the intramolecular association dominant in the dilute regime. The effectiveness and sustainability of these hydrophobic interactions is enhanced when operating below a critical separation concentration value where the balance of molecular interactions is sustained. This sustainability ensures that there are sufficient hydrophobic interactions propagated in the centre of the pores, which enhances the mobility control of the polymers. This work has demonstrated this effect by investigating the interplay between hydrophobic interactions and porous media. Other vital deliverables achieved by this

work include the quantification of hydrophobic interactions in the semi-dilute regime and intramolecular interactions in the dilute regime using dimensionless parameters defined based on suitable theoretical assumptions. This quantification procedure allows for a clear numerical indication of the difference in the proportion of molecular interactions between the dilute and the semi-dilute regime. Also, it was established in this work that the critical separation concentration where this balance is maintained is affected by the reservoir conditions. In other words, the value of the critical separation concentration tends to increase with temperature and brine salinity. This increment is simply an indication there is a direct relationship between the reservoir conditions and the critical separation concentration. Similarly, the significance of this novel optimization approach is the control, monitoring and prediction of the sustainability of hydrophobic interactions under different reservoir conditions. This can be translated or adjusted for in the required polymer concentration for oil recovery operations. However, other factors such as pore structure of a porous media may play an essential role in the determination of the critical separation concentration for the use of associative polymers. The effect of the pore structure is manifested in length (L) and radius of pore throat (R), the diameter of the expansion channel (D), contraction ratio (D/2R) and length to the radius of contraction (L/R).

Nomenclature

Abbreviations

CAC	Critical Aggregation Concentration
TDS	Total Dissolved Solids
EOR	Enhanced Oil Recovery

Symbols

B_s	Brine Salinity, **mg/L**
C_c	Critical Aggregation Concentration, **g/L**

$(C_c)_{T,B_s}$	Critical Concentration at different at Conditions of γ, B_s and T, **g/L**
C_p	Polymer Concentration, **g/L**
I_d	Dimensionless Parameter for Intramolecular Interactions
$(I_d)_{T,B_s}$	Intramolecular interactions at different at Conditions of γ, B_s and T, **g/L**
$C_{p,opt}$	Critical Separation Concentration, **g/L**
I_{sd}	Dimensionless Parameter for Hydrophobic Interactions
$(I_{sd})_{T,B_s}$	Hydrophobic Interactions at Reservoir Conditions of γ, B_s and T
T	Temperature, ℃
$\bar{M}_w$	Molecular Weight of Polymer, **g/mol**
γ	Shear Rate, **1/s**
μ_p	Polymer Vscosity, **Pas**

Acknowledgement

The authors would like to acknowledge the financial grant (PTDF/ED/PHD/ARO/1387/18) from the Petroleum Technology Development Fund (PTDF) Nigeria for this research work. Also, the authors acknowledge the comments and contributions of the various anonymous reviewers of this article.

Conflict of Interest

The authors declare that there is no conflict of interest regarding the publication of this article.

References

Afolabi, R. O. (2015). Effect of Surfactant and Hydrophobe Content on the Rheology of Poly(acrylamide-co-N-dodecylacrylamide) for Potential Enhanced Oil Recovery Application. *American Journal of Polymer Science*, *5*(2), 41-46.

Afolabi, R. O., Oluyemi, G. F., Officer, S., & Ugwu, J. O. (2019a). Hydrophobically Associating Polymers for Enhanced Oil Recovery – Part A: A Review on the Effect of Some Key Reservior Conditions. *Journal of Petroleum Science and Engineering, 180,* 681-698.

Afolabi, R. O., Oluyemi, G. F., Officer, S., & Ugwu, J. O. (2019b). Hydrophobically Associating Polymers for Enhanced Oil Recovery – Part B: A Review of Modelling Approach to Flow in Porous Media. *Journal of Molecular Liquids, 293,* 1-14.

Afolabi, R. O. & Yusuf, E. O. (2019). Nanotechnology and the Global Energy Demand: Challenges and Prospects for a Paradigm Shift in the Oil and Gas Industry. *Journal of Petroleum Exploration and Production Technology, 9(2),* 1423-1441.

Chen, H., Tang, H., Wu, X., Liu, Y., Bai, J., & Zhao, F. (2016). Synthesis, Characterization, and Property Evaluation of a Hydrophobically Modified Polyacrylamide as Enhanced Oil Recovery Chemical. *Journal of Dispersion Science and Technology, 37*(4), 486–495.

Gou, S., Luo, S., Liu, T., Zhao, P., He, Y., Pan, Q., & Guo, Q. (2015). A Novel Water- Soluble Hydrophobically Associating Polyacrylamide Based on Oleic Imidazoline and Sulfonate for Enhanced Oil Recovery. *New Journal Chemistry, 39,* 7805-7814.

Khan, N., & Brettmann, B. (2019). Intermolecular Interactions in Polyelectrolyte and Surfactant Complexes in Solution. *Polymer, 11*(1), 1-28.

Li, X., Shu, Z., Luo, P., & Ye, Z. (2018). Associating Polymer Networks Based on Cyclodextrin Inclusion Compounds for Heavy Oil Recovery. *Journal of Chemistry, 2018,* 1-9.

Liu, R., Pu, W., Jia, H., Shang, X., Pan, Y., & Yan, Z. (2014). Rheological Properties of Hydrophobically Associative Copolymers Prepared in a Mixed Micellar Method Based on Methacryloxyethyl-dimethyl Cetyl Ammonium Chloride as Surfmer. *International Journal of Polymer Science, 2014,* 1-14.

Quan, H., Li, Z., & Huang, Z. (2016). Self-assembly Properties of a Temperature- and Salt-Tolerant Amphoteric Hydrophobically Associating Polyacrylamide. *RSC Advances, 6,* 49281-49288.

Sun, J., Du, W., Pu, X., Zou, Z., & Zhu, B. (2015). Synthesis and Evaluation of a Novel Hydrophobically Associating Polymer Based on Acrylamide for Enhanced Oil Recovery. *Chemical Papers*, *69*(12), 1598–1607.

Yang, T., Choi, S. K., Lee, Y. R., Cho, Y., & Kim, J. W. (2016). Novel Associative Nanoparticles Grafted with Hydrophobically Modified Zwitterionic Polymer Brushes for the Rheological Control of Aqueous Polymer Gel Fluids. *Polymer Chemistry*, *7*(20), 3471-3476.

Ye, Z., Feng, M., Gou, S., Liu, M., Huang, Z., & Liu, T. (2013). Hydrophobically Associating Acrylamide- Based Copolymer for Chemically Enhanced Oil Recovery. *Kournal of Applied Polymer Science*, *130*(4), 2901-2911.

Zhang, Y., Mao, J., Zhao, J., Yang, X., Xu, T., Lin, C., . . . Ma, S. (2019). Preparation of a Hydrophobic-Associating Polymer with Ultra-High Salt Resistance Using Synergistic Effect. *Polymers*, *11*(4), 1-18.

Zhong, H., Li, Y., Zhang, W., Yin, H., Lu, J., & Guo, D. (2018). Microflow Mechanism of Oil Displacement by Viscoelastic Hydrophobically Associating Water-Soluble Polymers in Enhanced Oil Recovery. *Polymers*, *10*(6), 1-15.

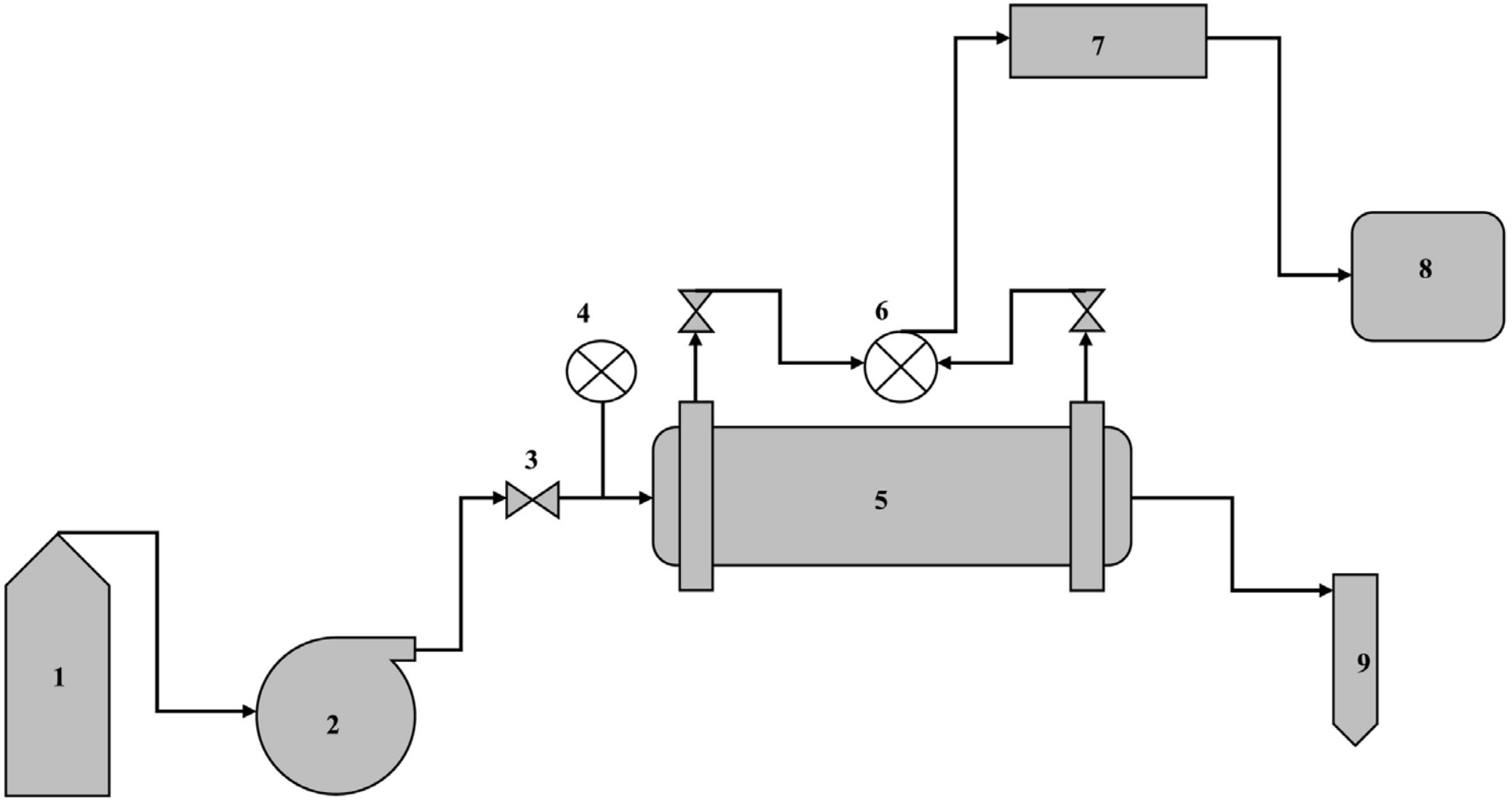

Figure 1*: Experimental setup of the core flooding apparatus. 1) pump fluid, 2) pump, 3) valves, 4) pressure gauge, 5) core holder with sand pack, 6) pressure transducer, 7) NIDAQ data logger, 8) desktop computer, 9) effluent sample collector (test tubes).*

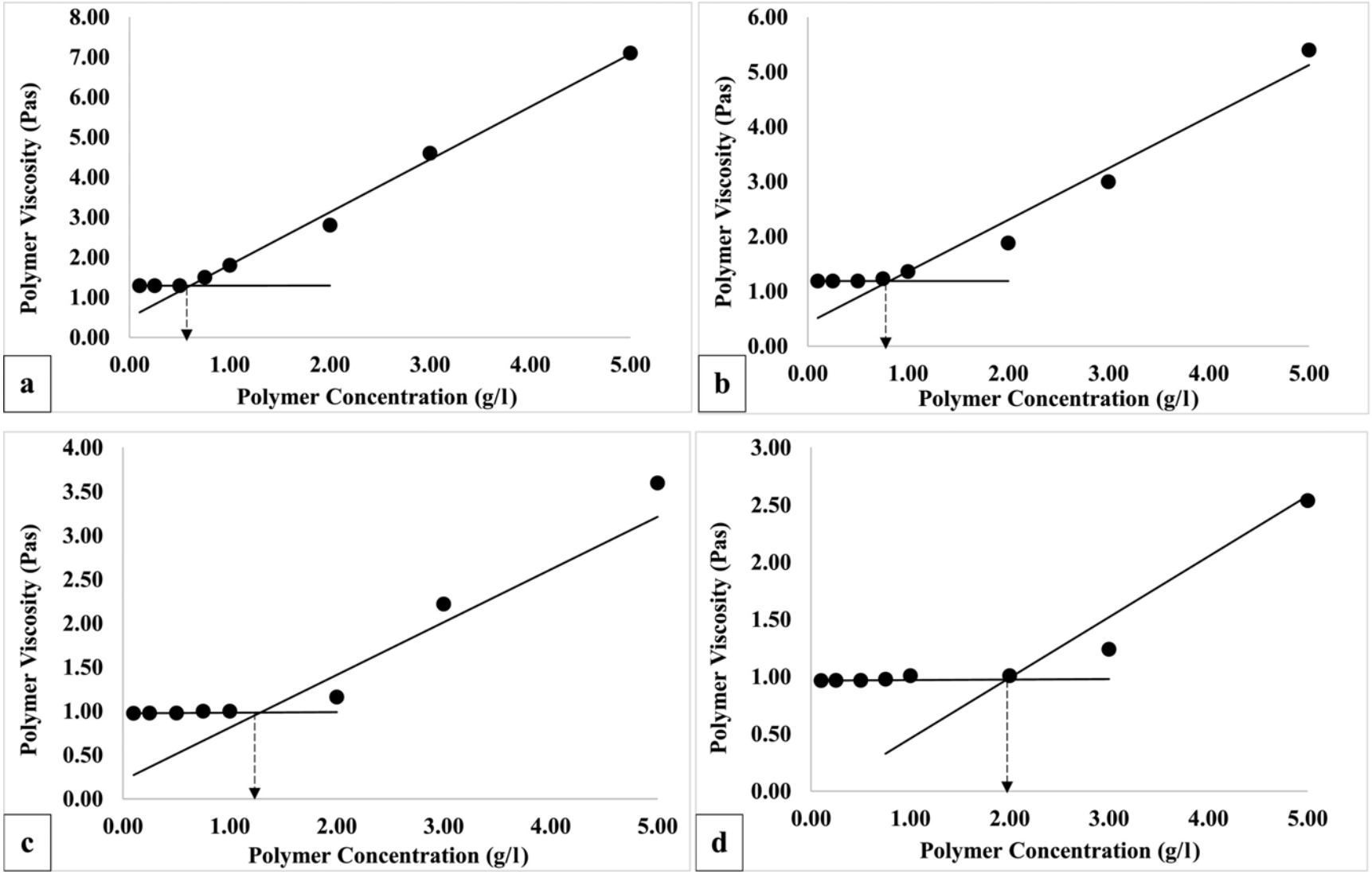

Figure 2: *Determination of the CAC from the plot of polymer viscosity against concentration at 3.6 % TDS and at low shear rate approximating zero-shear conditions (a) 25 ^{0}C (b) 50 ^{0}C (c) 75 ^{0}C (d) 85 ^{0}C.*

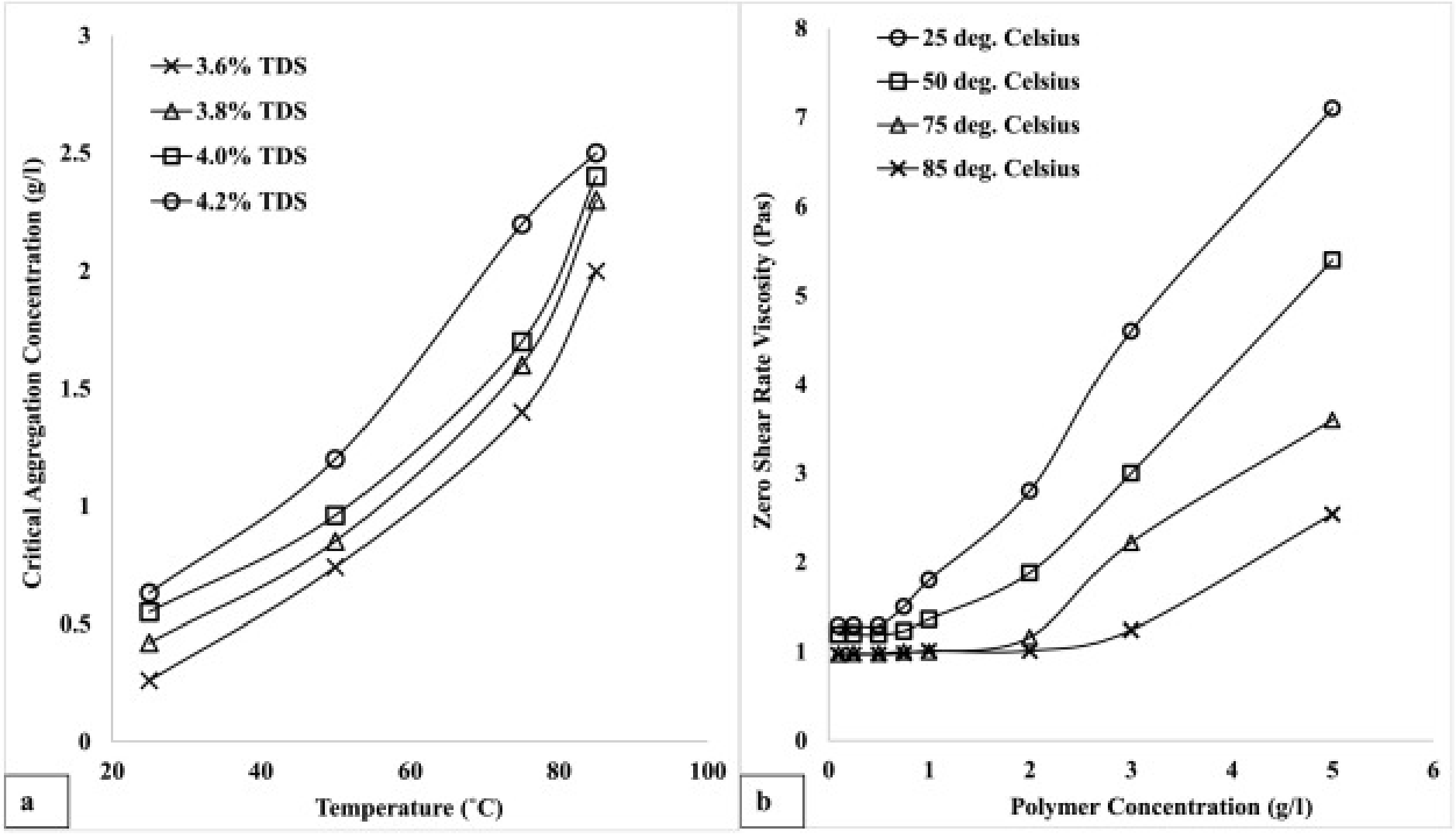

Figure 3*: (a) Effect of temperature on the critical aggregation concentration (CAC) at different %TDS. (b) Zero- shear viscosity profile at 3.6 %TDS from which the critical aggregation concentration were estimated using the linear method.*

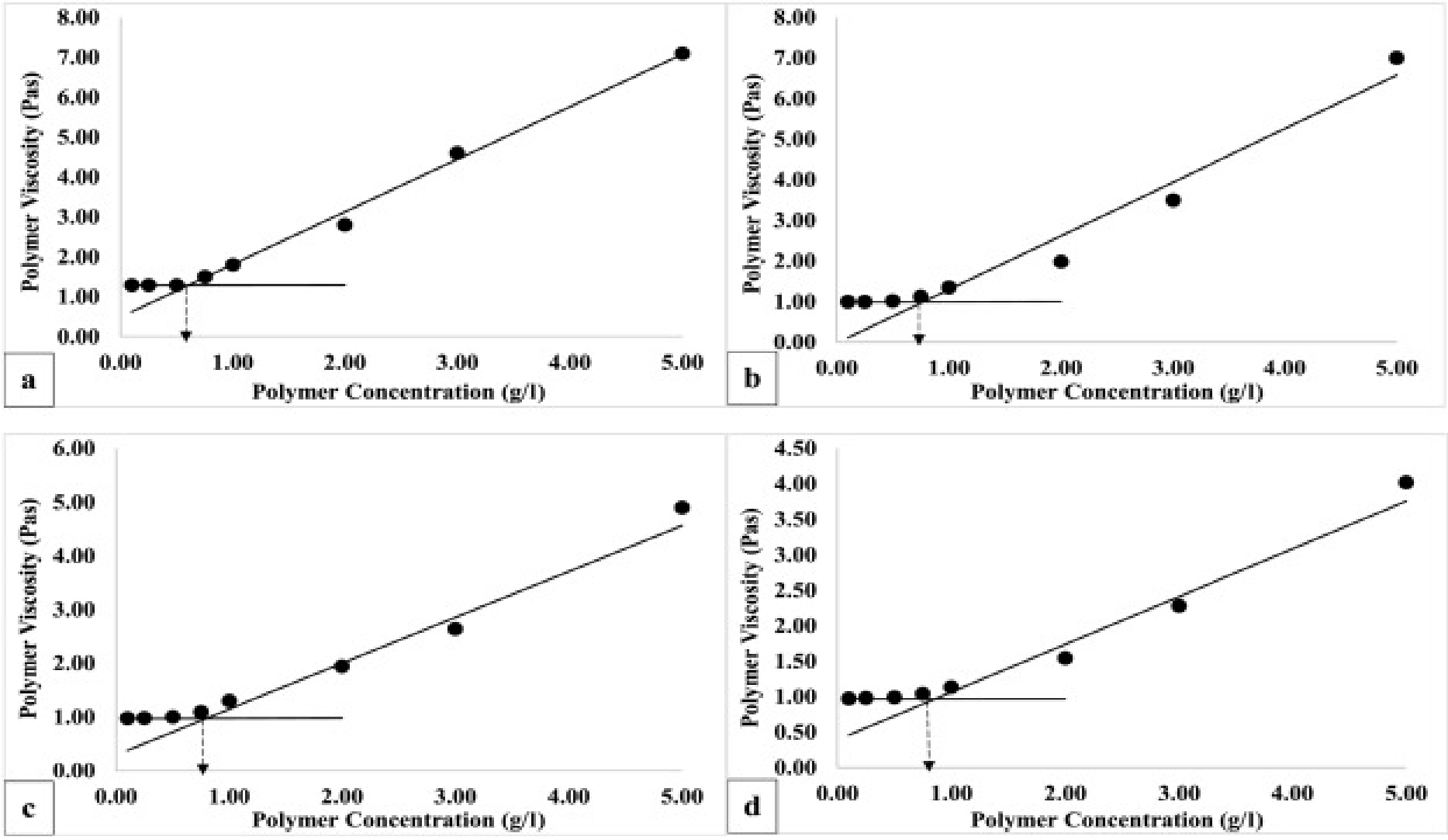

***Figure 4**: Determination of the CAC from the plot of polymer viscosity against concentration at 25 ^{0}C and low shear rate approximating zero-shear condition (a) 3.6 % TDS (b) 3.8 % TDS (c) 4.0 % TDS (d) 4.2 % TDS..*

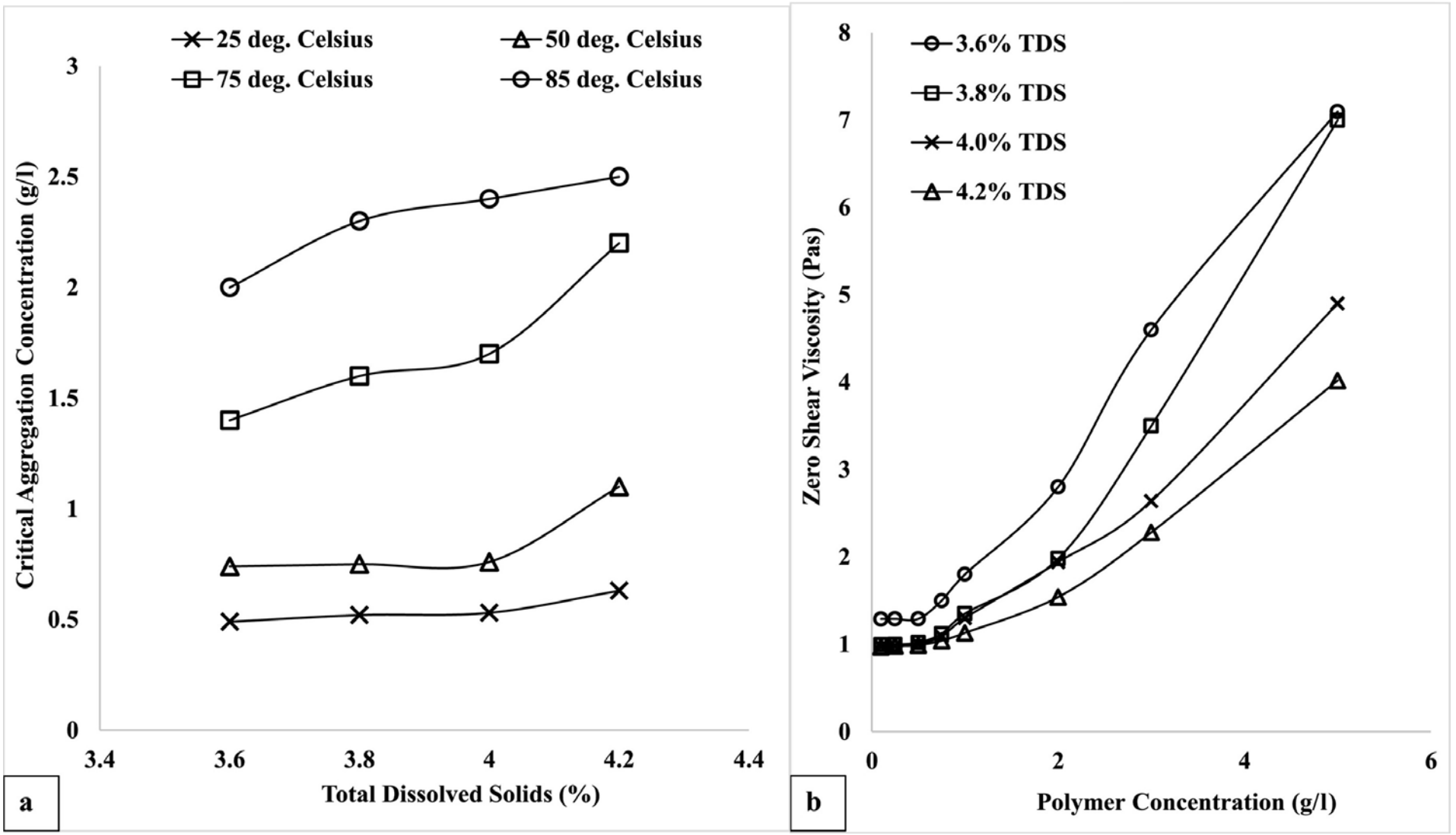

Figure 5*: (a) Effect of total dissolved solids on the critical aggregation concentration (CAC) at different temperatures. (b) Zero-shear viscosity profile at 25 ℃ from which the critical aggregation concentration were estimated using the linear method.*

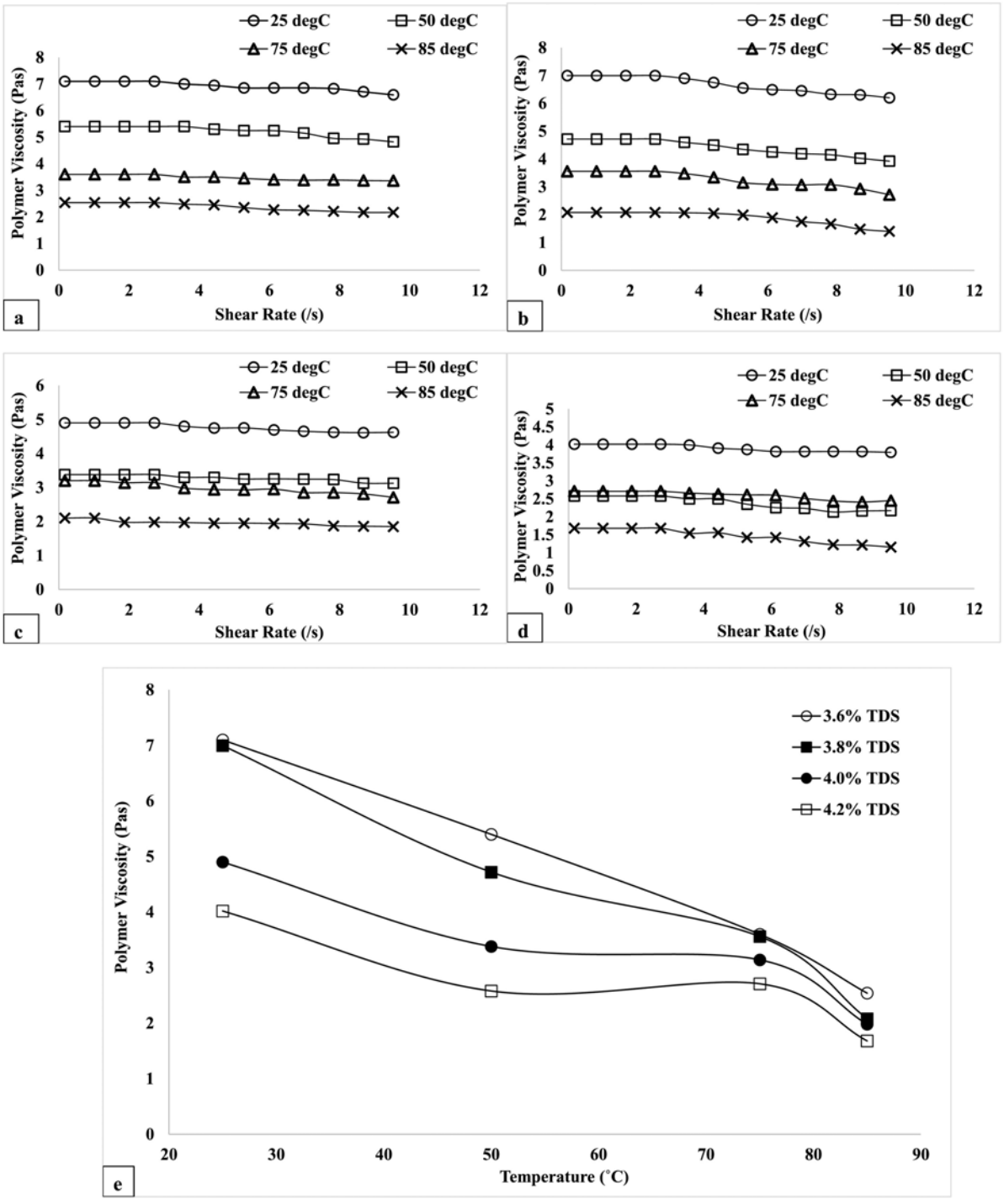

***Figure 6**: The plots of polymer viscosity variation with shear rate at given temperatures for 5 g/L polymer solution. The plots were generated at different conditions of total dissolved solids: (a) 3.6 %TDS (b) 3.8 %TDS (c) 4.0 %TDS (d) 4.2 %TDS (e) Summary of the effect of temperature on the polymer viscosity at the lowest shear rate approximating zero-shear condition.*

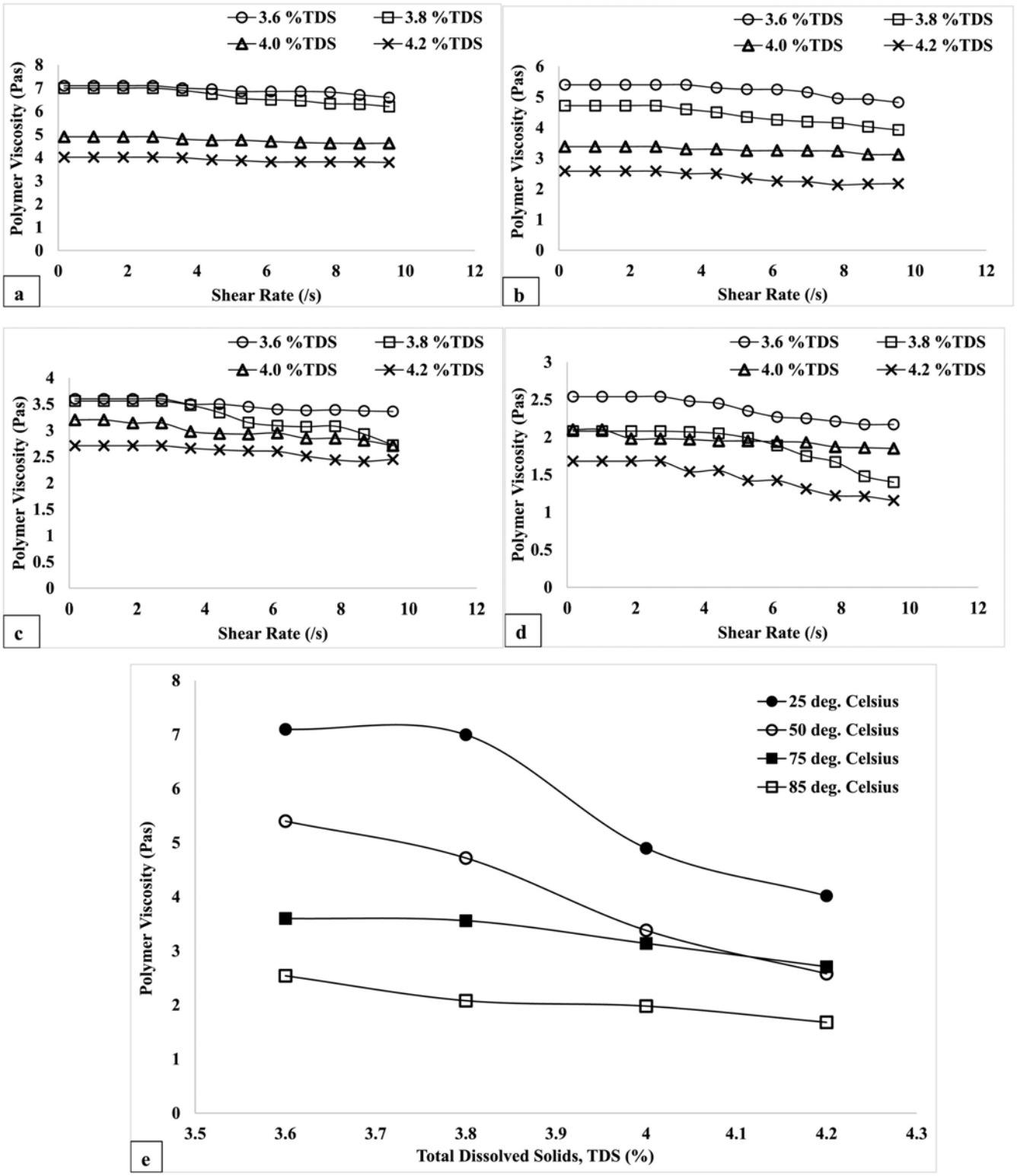

Figure 7*: The plots of polymer viscosity variation with shear rate at given total dissolved solids for 5 g/L polymer solution. The plots were generated at different conditions of temperatures: (a) 25 ℃ (b) 50 ℃ (c) 75 ℃ (d) 85℃ (e) Summary of the effect of total dissolved solids on the polymer viscosity at lowest shear rate approximating zero-shear condition.*

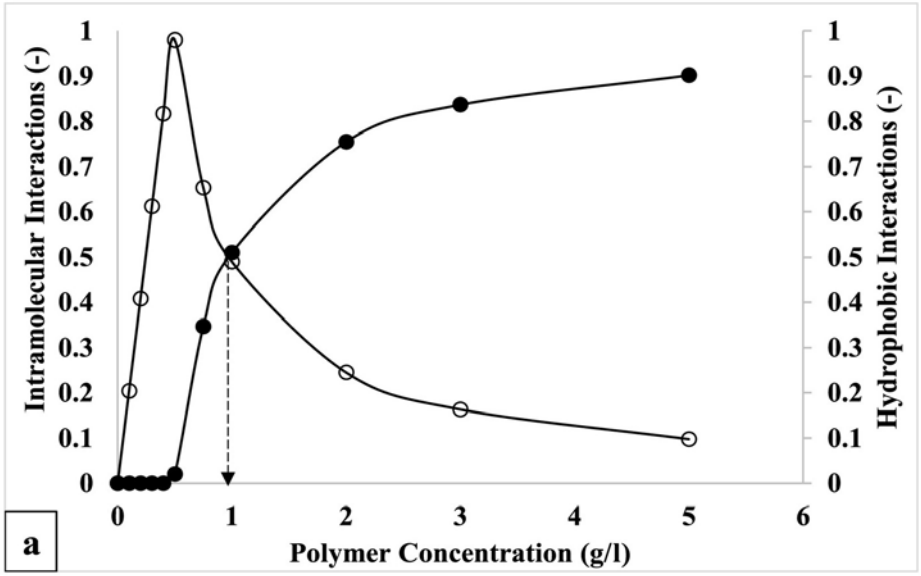
Intramolecular Interactions (-)
Hydrophobic Interactions (-)
Polymer Concentration (g/l)
a

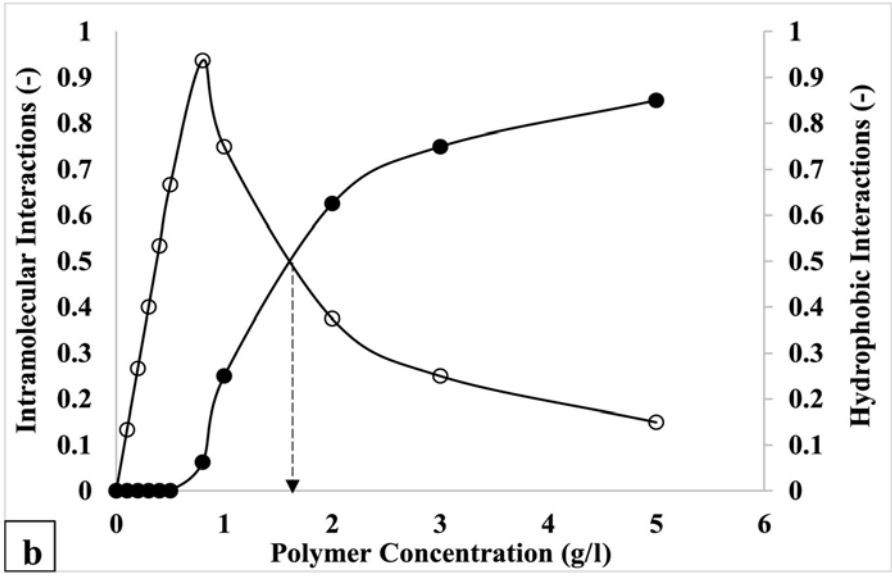
Intramolecular Interactions (-)
Hydrophobic Interactions (-)
Polymer Concentration (g/l)
b

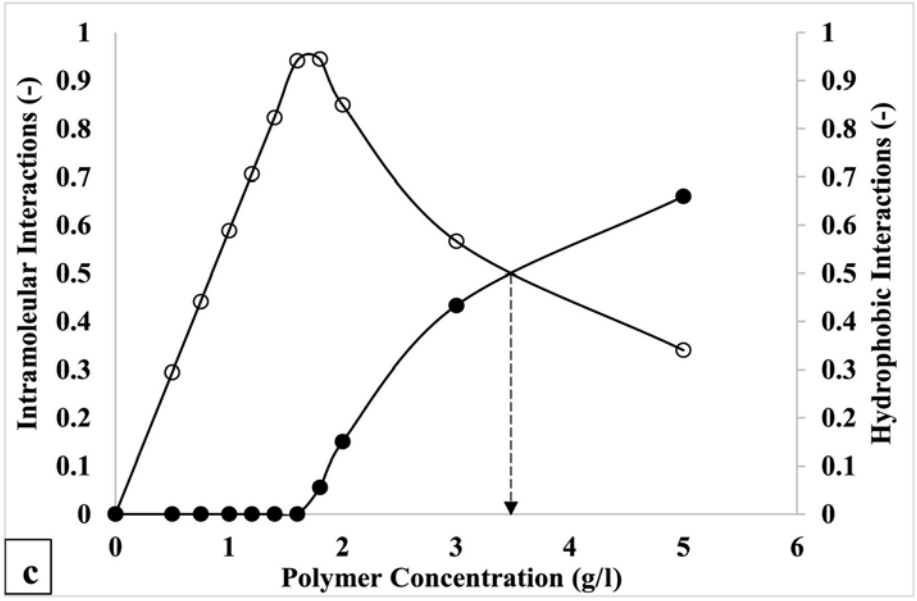
Intramoleular Interactions (-)
Hydrophobic Interactions (-)
Polymer Concentration (g/l)
c

Figure 8: *Plot of intramolecular interaction and hydrophobic interaction against polymer concentration at (a) 25 °C (3.6 % TDS) (b) 50 °C (3.8 % TDS) (c) 75 °C (4.0 % TDS). The critical separation concentrations at each condition are shown below.*

Intramolecular Interactions – ○

Hydrophobic interactions – ●.

Temperature (℃) and polymer concentration

25 ^{0}C (3.6 % TDS)
50 ^{0}C (3.8 % TDS)
75 ^{0}C (4.0 % TDS)

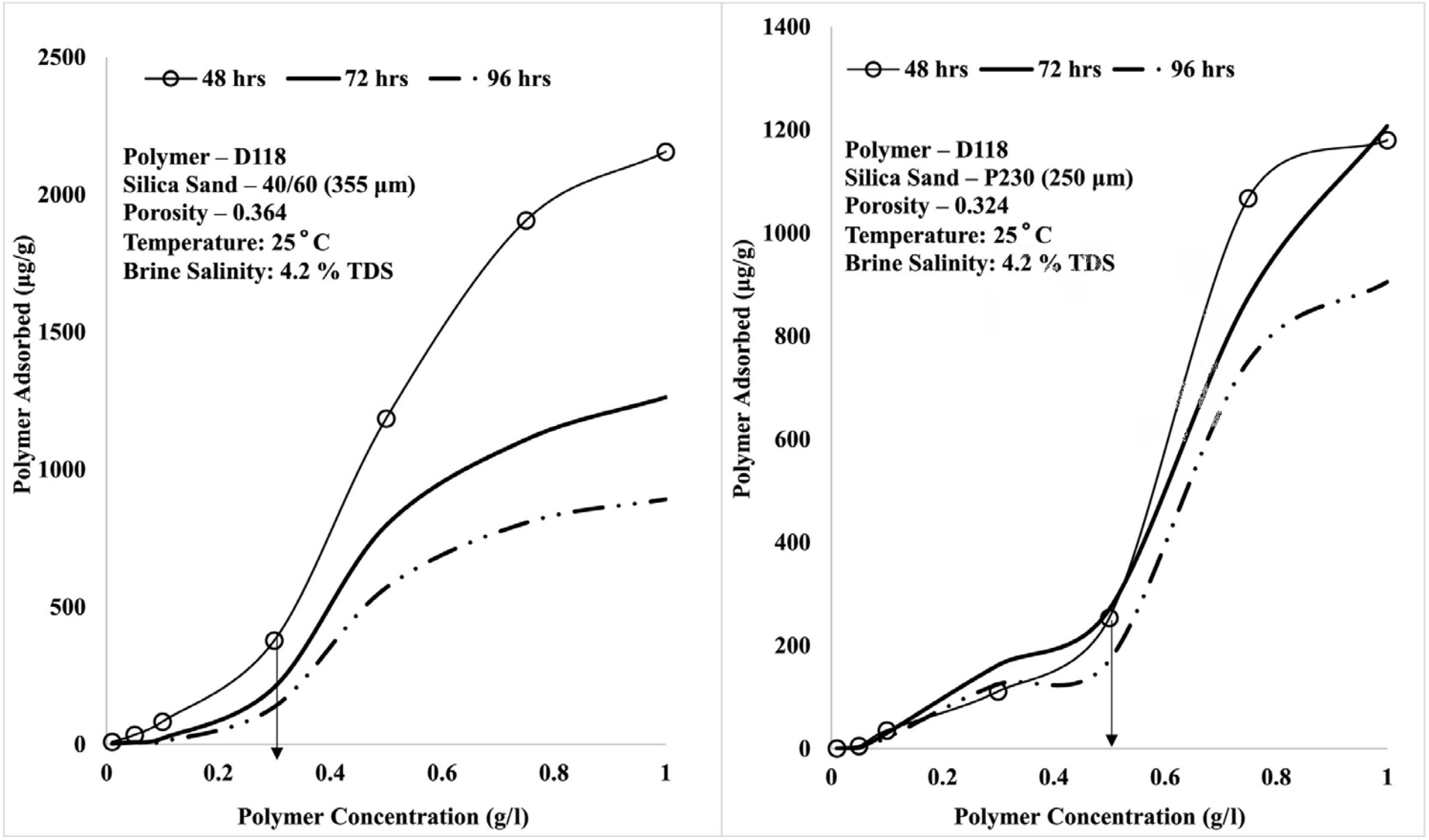

Figure 9: *Plot of polymer adsorbed against concentration after contacting in different commercial silica sands (a) Silica sand – 40/60 (b) Silica sand – P230.*

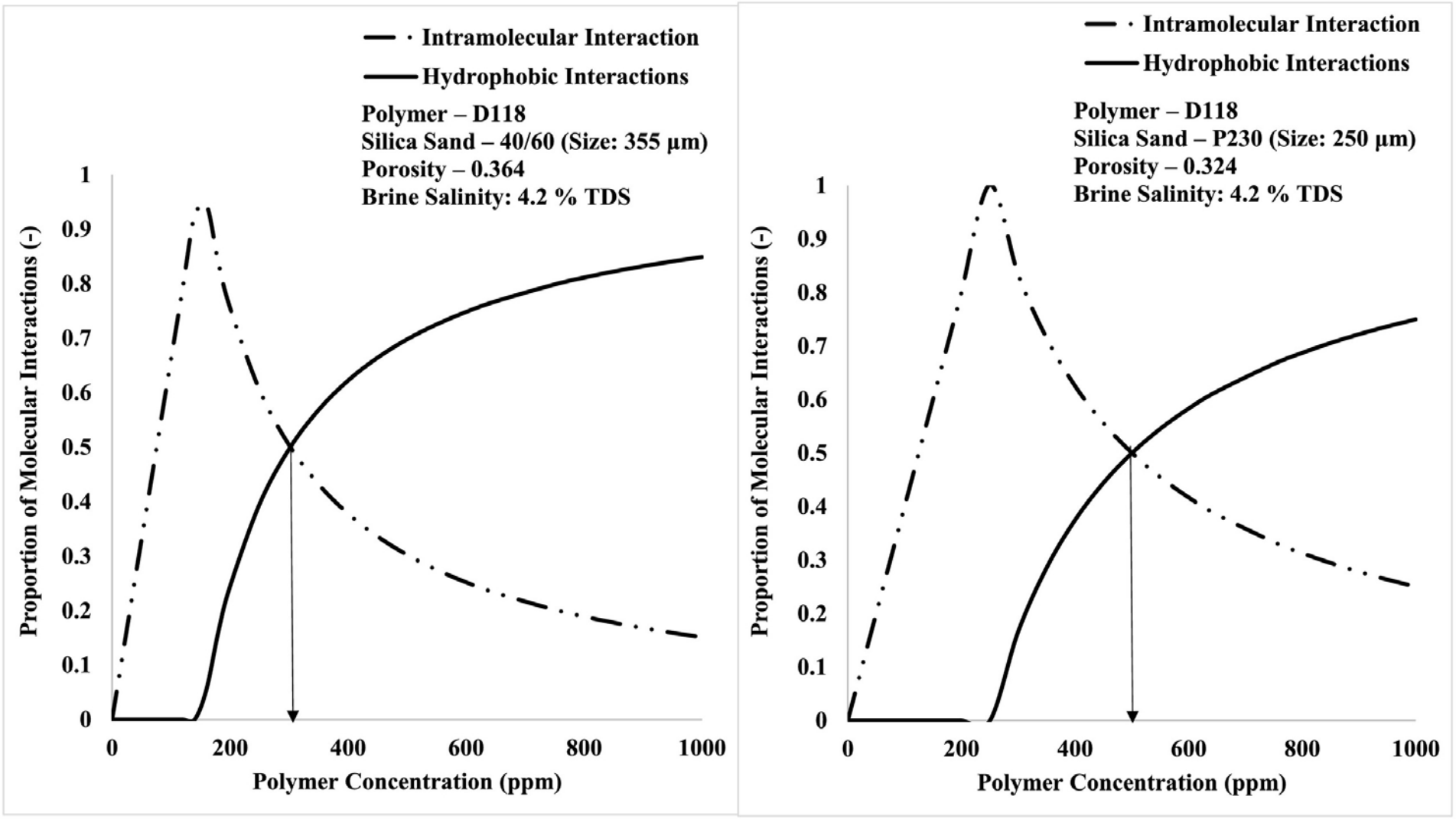

Figure 10: *Plot of molecular interactions against polymer concentration (a) Silica sand – 40/60 (b) Silica sand – P230.*

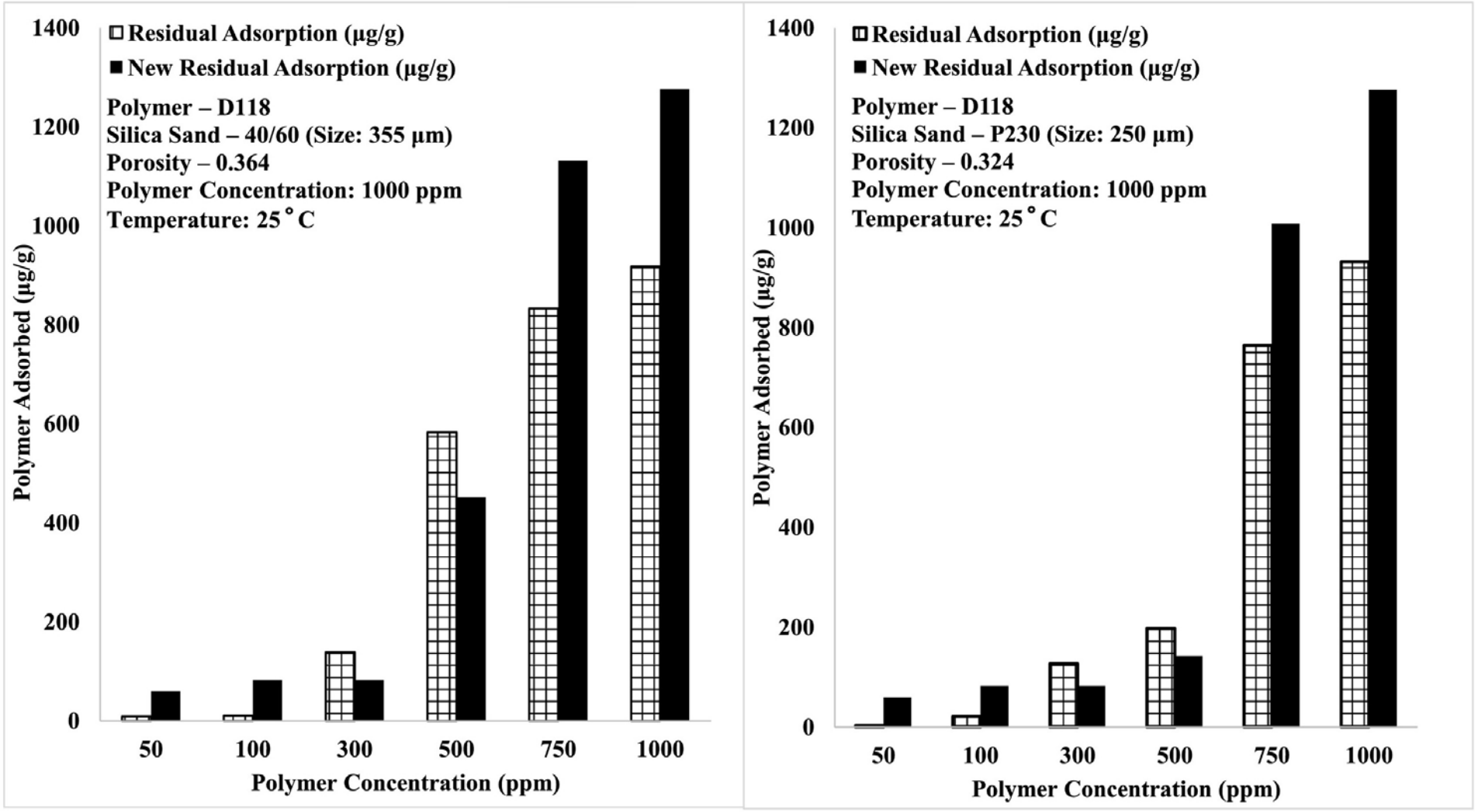

Figure 11: *Polymer re-adsorption process by contacting 1000 ppm of polymer solution with initially contacted sand (a) Silica sand - 40/60 (b) Silica sand - P230.*

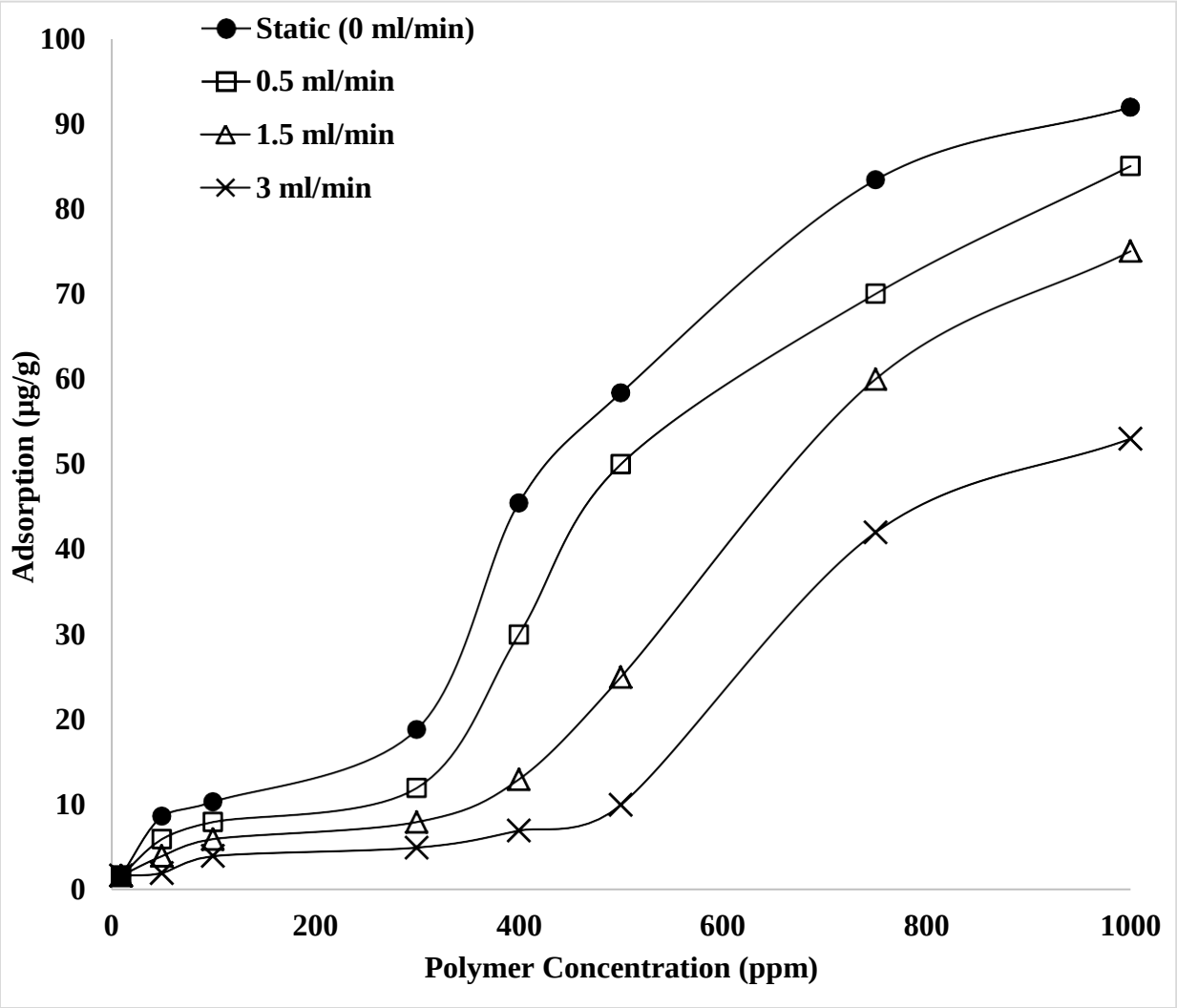

***Figure 12**: Effect of flow conditions (flow rate) on the dynamic adsorption of associative polymer in the 40/60 silica sand ($\phi = 0.364; k = 147\ mD$) at 4.2 %TDS and 25 ℃.*

***Table 1**: Synthetic brine composition for samples S_1 to S_4 prepared at 25 ^{0}C. The pH values for the brine samples S_1 to S_4 are 7.58, 7.92, 7.83 and 7.88 respectively.*

Composition of Synthetic Formation Brine				
Compound	**S_1 (wt.%)**	**S_2 (wt.%)**	**S_3(wt.%)**	**S_4(wt.%)**
Sodium Chloride, **NaCl**	2.266	2.553	2.739	2.925
Magnesium Chloride, **$MgCl_2$**	0.500	0.500	0.499	0.499
Sodium Sulphate, **Na_2SO_4**	0.394	0.394	0.394	0.393
Calcium Chloride, **$CaCl_2$**	0.236	0.255	0.275	0.294
Potassium Chloride, **KCl**	0.067	0.066	0.066	0.066
Sodium Hydrogen Carbonate, **$NaHCO_3$**	0.019	0.019	0.019	0.019
Strontium Chloride, **$SrCl_2$**	0.002	0.002	0.002	0.002
Total Dissolved Solids (TDS)	3.586	3.792	3.995	4.198

***Table 2**: Calculation procedure employed in the preparation of stock and dilute polymer solutions according to the API specification RP-63 (Recommended Practices for Evaluation of Polymers for Enhanced Oil Recovery).*

Experimental Procedure	**Equation**	**Variable Description**
Determination of Activity of Polymer Product	$A_{pr} = \frac{W_{d+DS} - W_d}{W_{d+HS} - W_d} \text{x } 100$	A_{pr} = Activity of Polymer Product W_d = Wight of empty ceramic dish, g; W_{d+DS} = Weight of dish and polymer, g; W_{d+HS} = Weight of dish and polymer after heating and cooling, g.
Preparation of Stock Polymer Solution (5000 ppm)	$W_{pr} = \frac{W_s \text{ x } C_s \text{ x } 10^{-4}}{A_{pr}}$	W_{pr} = weight of polymer product, g W_s = weight of stock solution to be made, g C_s = concentration of polymer in stock solution, ppm A_{pr} = activity of the polymer product, wt.%
	$W_{bs} = W_s - W_{pr}$	W_{bs} = Amount of make-up water, g
Preparation of Dilute Polymer Solution	$W_s = \frac{W_d \text{ x } C_{dl}}{C_s}$	W_d = weight of diluted solution to be made, g. C_{dl} = concentration of polymer in diluted solution, ppm.
	$W_{bd} = W_d - W_s$	W_{bd} = weight of makeup water used in the diluted solution, g.

***Table 3**: Composition and properties of the commercial sands employed and synthetic brine. The synthetic brine composition was at 25 ^{0}C with pH value and specific gravity of 7.88 and 1.02 respectively.*

Synthetic Formation Brine						
Composition	**NaCl**	**KCl**	**$CaCl_2$**	**$MgCl_2$**	**Na_2SO_4**	**$NaHCO_3$**
Quantity (mg/L)	40,000	1,000	4,000	5,000	1,000	200

Commercial Silica Sand Properties				
Code Name	**Grain Density (g/cm^3)**	**Porosity**	**Average Grain Diameter (µm)**	**Main Component**
40/60	1.724	0.364	355	Quartz (> 99.9%)
P230	1.672	0.324	250	Quartz (> 99.9%)

Authors Statement

Richard O. Afolabi: Conceptualization, Methodology, Formal Analysis, Investigation, Writing - Original Draft. **Gbenga F. Oluyemi**: Supervision, Conceptualization, Validation, Review and Editing, Project Administration. **Simon Officer**: Supervision, Conceptualization, Project Administration, Review and Editing. **Johnson O. Ugwu**: Supervision, Project Administration, Review.

Declaration of Interests

The authors declare that they have no known competing financial interests or personal relationships that could have appeared to influence the work reported in this paper.

Highlights

- A dimensionless parameter for the numerical quantification of hydrophobic interactions.
- Modelling the variation in hydrophobic interactions arising from oil reservoir conditions.
- Prediction of a critical separation concentration for associative polymers.
- Sustainability of hydrophobic interactions between associative polymers in porous media.